J. Physiol. (1970), **211**, *pp.* 729–751
With 12 *text-figures*
Printed in Great Britain

SODIUM AND POTASSIUM CONDUCTANCE CHANGES DURING A MEMBRANE ACTION POTENTIAL

By FRANCISCO BEZANILLA,* EDUARDO ROJAS and ROBERT E. TAYLOR

From the Faculty of Sciences, University of Chile, Clasificador 198, Correo Central, Santiago, Chile and the Laboratory of Biophysics, National Institute of Neurological Diseases and Stroke, National Institutes of Health, Bethesda, Maryland, U.S.A.

(*Received 29 June 1970*)

SUMMARY

1. A method for turning a membrane potential control system on and off in less than 10 μsec is described. This method was used to record membrane currents in perfused giant axons from *Dosidicus gigas* and *Loligo forbesi* after turning on the voltage clamp system at various times during the course of a membrane action potential.

2. The membrane current measured just after the capacity charging transient was found to have an almost linear relation to the controlled membrane potential.

3. The total membrane conductance taken from these current–voltage curves was found to have a time course during the action potential similar to that found by Cole & Curtis (1939).

4. The instantaneous current voltage curves were linear enough to make it possible to obtain a good estimate of the individual sodium and potassium channel conductances, either algebraically or by clamping to the sodium, or potassium, reversal potentials. Good general agreement was obtained with the predictions of the Hodgkin–Huxley equations.

5. We consider these results to constitute the first direct experimental demonstration of the conductance changes to sodium and potassium during the course of an action potential.

* Fellow of the Comisión Nacional de Investigación Científica y Tecnológica, Chile. Present address: Department of Physiology, University of Rochester, Rochester, N.Y., U.S.A.

INTRODUCTION

Our present ideas concerning the ionic nature of the action potential are based on the results of many experiments utilizing a variety of cells, particularly giant nerve fibres (Cole, 1968). The presentation of the sodium-potassium nerve model by Hodgkin & Huxley in 1952 very elegantly accounted for most of the information available at that time and provided a challenge to test its predictions. In 1939, Cole & Curtis measured a transient change in membrane impedance (at 20 kc) concomitant with the action potential which was shown to be mainly due to a change in membrane conductance. Hodgkin & Huxley calculated the time course of the sodium and potassium conductance change during the course of an action potential and made the total conductance change equal to the sum of these two conductances plus a small leakage. They showed that the time course of the calculated conductance change was very similar to the time course measured by Cole & Curtis (Hodgkin & Huxley, 1952, Fig. 16). However, it has not been possible to measure separately the individual components (sodium and potassium) of this total conductance even though considerable attention has been given to this problem (Weidmann, 1951; Vassalle, 1966; Morlock, Benamy & Grundfest, 1968; Peper & Trautwein, 1969).

This paper presents the results of experiments in which the sodium and potassium conductance changes postulated by Hodgkin & Huxley were measured during the course of an action potential. The method which we used to separate these conductances from the total conductance is accurate only if the instantaneous current–voltage curve at any time during the course of a membrane action potential is linear. We present evidence that for squid giant axons from *Dosidicus gigas* and from *Loligo forbesi* the departure of the instantaneous current–voltage curve from linearity is not serious over the relevant potential range.

A preliminary report of this paper has been published elsewhere (Rojas, Bezanilla & Taylor, 1970).

METHODS

Giant axons from the squid *Dosidicus gigas*, available at the Laboratorio de Fisiología Celular, Universidad de Chile, Montemar, Chile, and from *Loligo forbesi*, available at the Laboratory of the Marine Biological Association, Plymouth, England, were used in this work. A description of the arrangement used for intracellular perfusion has been presented before (Rojas, Taylor, Atwater & Bezanilla, 1969).

Proper membrane potential control (or membrane current control) implies a 'space clamp' (Cole, 1968). Ideally there would be no variations of membrane potential with distance along the length of the axon in the measuring region and in practice this condition is closely approximated (Rojas *et al.* 1969). A 'membrane action potential' is an action potential produced under these space clamp conditions

with no net current flow across the membrane except for a brief shock used to initiate the activity. During this action potential the properties of the membrane are changing with time. Fig. 1 represents a simplified diagram of the arrangement for membrane potential or membrane current control. If at a given time during the course of the action potential (Fig. 1, left side), the membrane potential is suddenly controlled (voltage clamp) the membrane current is not zero and has the time course shown in Fig. 1, right side.

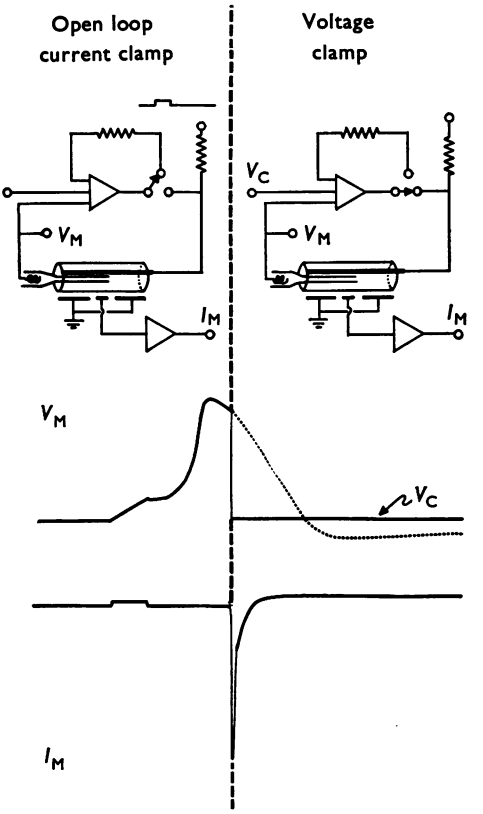

Fig. 1. Simplified diagram of the experimental procedure. Upper part: a simplified diagram of the system used to switch on the membrane potential control system. Lower part: the recorded membrane potential and membrane current. On the left side of the Figure the membrane is in open loop current clamp condition because the switch at the output of the control amplifier is connected to the auxiliary feed-back loop. The action potential is excited by a short pulse of voltage through a very high resistor connected to the axial wire. On the right side of the figure the switch connects the output of the control amplifier to the axial wire and the membrane is under voltage clamp condition. The free course of the action potential is interrupted and the recorded potential is equal to the command potential. Simultaneously membrane currents are recorded as shown in the bottom of the Figure.

At any given time the direction and the shape of the current record depend upon the time at which the voltage clamp interval was initiated and upon the value of the membrane potential during the control period.

For the experiment shown in Fig. 3, frame *b*, the control system was turned on at the time when the action potential was at its peak value. The upper traces represent the recorded membrane current and the lower traces represent the recorded membrane potential before and during the time at which the membrane potential was under control. The individual traces were taken at intervals of 1 sec for depolarizations from the resting potential (-60 mV) to -40 through $+100$ mV in 20 mV steps (potentials are referred to the external solution as zero; depolarizations and outward currents are positive). During the voltage clamp period with the membrane potential kept at V_c for

$$-60 \text{ mV} < V_c < +40 \text{ mV}$$

there is an inward current followed by an outward current. For

$$+40 \text{ mV} < V_c$$

the membrane current is always outward (although this is not shown in this particular record, when

$$V_c < -70 \text{ mV}$$

the membrane current is always inward). From these records it is possible to measure accurately the changes in membrane potential and the concomitant changes in membrane current. Such records were used to calculate the total membrane conductance just before the interruption and to separate the sodium and potassium conductance at any given time during the course of a membrane action potential.

Even though the method used to turn on the voltage clamp system is rather simple, a number of technical difficulties were encountered before obtaining a good performance. Fig. 2 is a diagram of the electrical circuit of the control system used.

The usual switch shown in Fig. 1 connecting the output of the control amplifier to either the current supplying wire (which is inside the fibre) or to the feed-back resistance was replaced by two transistors (a PNP transistor, 2N 3638 and a NPN transistor, 2N 3904). The collectors of these transistors are electrically connected together to the output of the control amplifier. The emitter of the NPN transistor is connected through a resistance to the input of the control amplifier. The emitter of the PNP transistor makes electrical contact with the current supplying wire. The bases are electrically connected together and to a positive constant voltage source which results in a high resistance between the emitter and the collector of the PNP transistor and a low resistance between the emitter and the collector of the NPN transistor; application of a negative rectangular voltage pulse to the bases reverses this situation and the membrane potential control system is turned on during the pulse. The change in resistance between the emitter and the collector resulting from the application of a negative voltage pulse is completed in less than 3 μsec provided that the pulse utilized is established in less than 3 μsec.

Current transients recorded with this system are fast. For example, it is very difficult to separate the capacitative current transient from the ionic current in the current transient shown in Fig. 3, second frame. A semilogarithmic plot of these currents as a function of time showed that in general the capacitative current falls off with a time constant of the order of 10 μsec and that the ionic current falls off with a time constant always greater than 100 μsec. The effect of a compensated feed-back system (correction for the voltage error due to the resistance in series with the axolemma, Hodgkin, Huxley & Katz, 1952) on the rate of fall of these transients is

shown in Fig. 8*A* and *B*. It can be seen that the current transients obtained with a compensated voltage clamp are faster than the current transients obtained without compensation.

Compensated feed-back was obtained by feeding a variable fraction, α, of the voltage output of the current amplifier into the summing point of the control amplifier (see Fig. 2). The degree of series resistance compensation achieved was measured in Ω cm^2 and was calculated as the ratio voltage difference between the recorded membrane potential with and without compensation/current density measured at the same time with compensation.

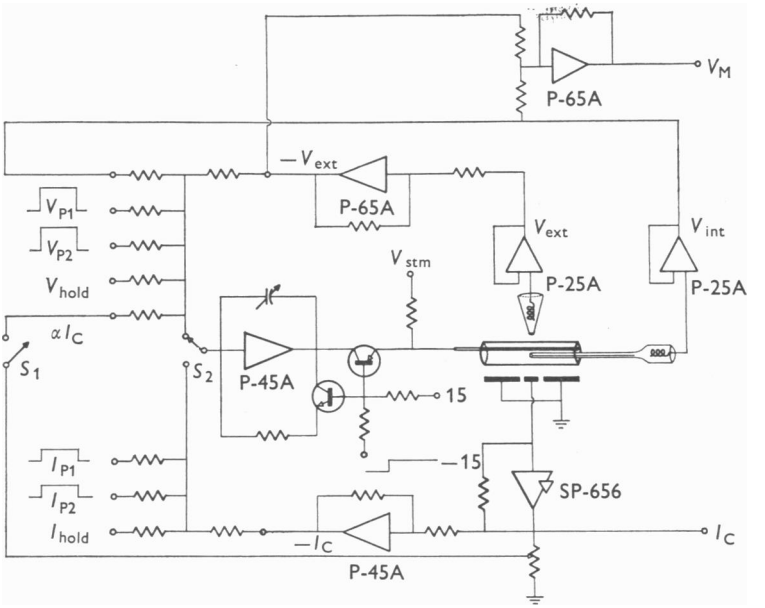

Fig. 2. Diagram of the voltage clamp system used. All operational amplifiers were from Philbrick. V_M: membrane potential; I_c: membrane current during clamp; S_1: switch used to obtain compensated feed-back; S_2: switch utilized to operate the system either as current clamp or voltage clamp. This switch can be replaced by a more sophisticated electronic switch made with FET transistors; NPN transistor: 2N 3904; PNP transistor 2N 3638. V_p: rectangular voltage pulses. I_p: rectangular current pulses. V_{hold}: holding potential. I_{hold}: holding current.

RESULTS

Instantaneous current–voltage relations during the course of a membrane action potential

Fig. 3 shows the results of an experiment in which the membrane potential control system was turned on 1·0, 1·3, 2·4 and 4·5 msec after the application of a depolarizing rectangular current pulse above threshold. In each frame the lower traces represent the recorded membrane potential

before and during the time in which the membrane potential was under control. The individual traces were taken at intervals of 1 sec for depolarizations from the resting potential (of -60 mV) to $+80$, $+100$ mV or $+120$ mV in 20 mV steps. Frame *a* shows the results obtained when the control system was turned on a bit after (1·0 msec) the application of the stimulating current (see stimulus artifact) and frame *d* illustrates the

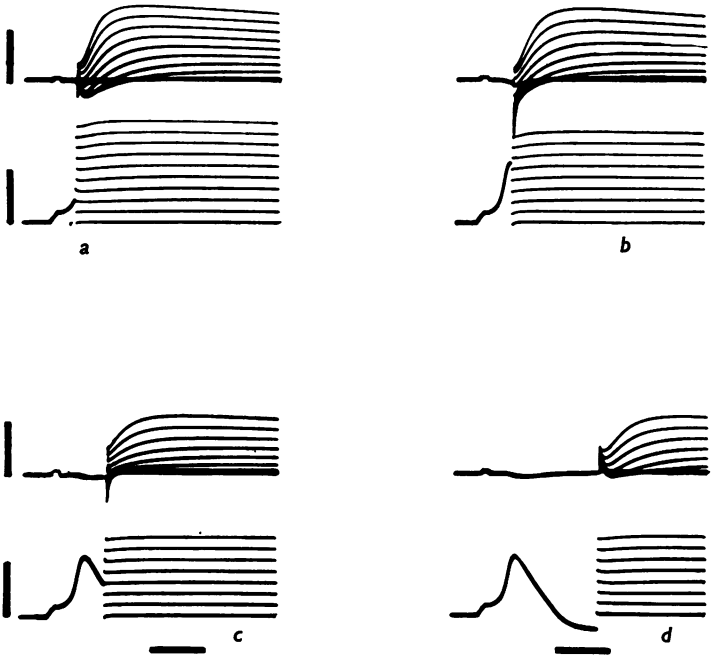

Fig. 3. Superimposed oscilloscope traces of membrane potentials and membrane currents before and during the voltage clamp period. Upper traces in each frame represent the recorded membrane currents and lower traces represent the recorded membrane potentials. (These records are not flat because compensated feed-back was used.) Calibrations: current: 2·68 mA/cm^2; voltage: 100 mV; time: 2 msec. *Dosidicus* axon. Resting potential -60 mV; Temperature: 8° C.

results obtained when the control system was turned on almost at the end of the action potential (4·5 msec). The voltage traces are not flat because the controlled membrane potential was corrected for the voltage drop across 4 Ω cm^2 of series resistance. The following is apparent from these records:

(I) If the control system is turned on before the initiation of the action potential, current records for different depolarizations have their usual shape; after completion of the capacitative current transient, the initial current is in the inward direction and the delayed current is outward.

(II) Steady-state currents are quite independent of the time at which the control system is turned on. The shape of the inward current, on the other hand, depends on the time at which the control system is turned on. This point is best illustrated by the results presented in Fig. 4 where the membrane potential was controlled at -40 mV and the resting potential was -60 mV. Upper traces show the membrane currents and lower traces show the recorded membrane potential. The inward currents change from

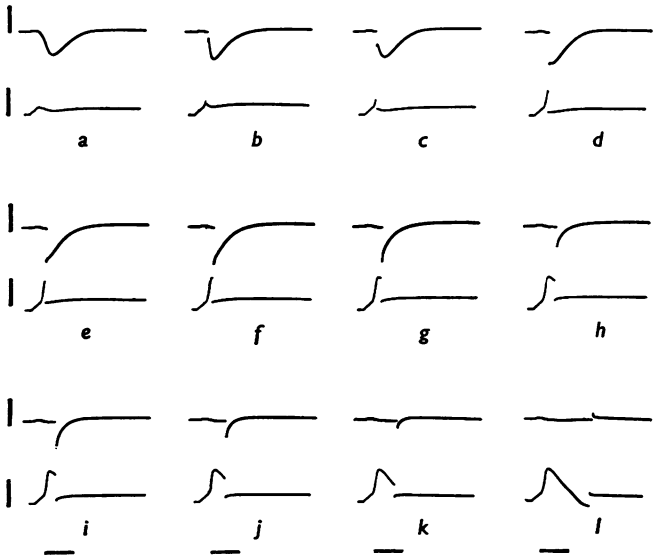

Fig. 4. Action potential interruption to -40 mV. At a given controlled potential, the shape of the early current depends upon the time at which the voltage clamp interval was initiated. Upper traces represent the recorded membrane currents. Lower traces represent the recorded membrane potential. Resting potential was -60 mV. Calibrations: current: 3 mA/cm^2; voltage: 100 mV; time: 2 msec. *Dosidicus* axon at 12° C.

their usual shape (frame *a*) to that of a 'tail' of inward current (from frame *d* to frame *k*). The characteristic of the recorded membrane currents suggests that as in the case of a regular voltage clamp pulse the inward currents are carried by sodium ions and that the delayed outward currents are carried by potassium ions, which is the only cation present in the perfusing solution (Atwater, Bezanilla & Rojas, 1969; Bezanilla, Rojas & Taylor, 1970).

From records of the type shown in Fig. 3 it is possible to measure the initial membrane current 30 μsec after the control system is turned on and plot these currents against the membrane potential during the control period. We consider that after this time the membrane capacity has been

charged and that the measured current is ionic current. The results of six experiments are shown in Fig. 5*A* and *B*. The time (after the beginning of the stimulating current pulse) during the course of the membrane action potential at which each curve was measured is given next to the corresponding current–voltage curve. It is apparent from these curves that there

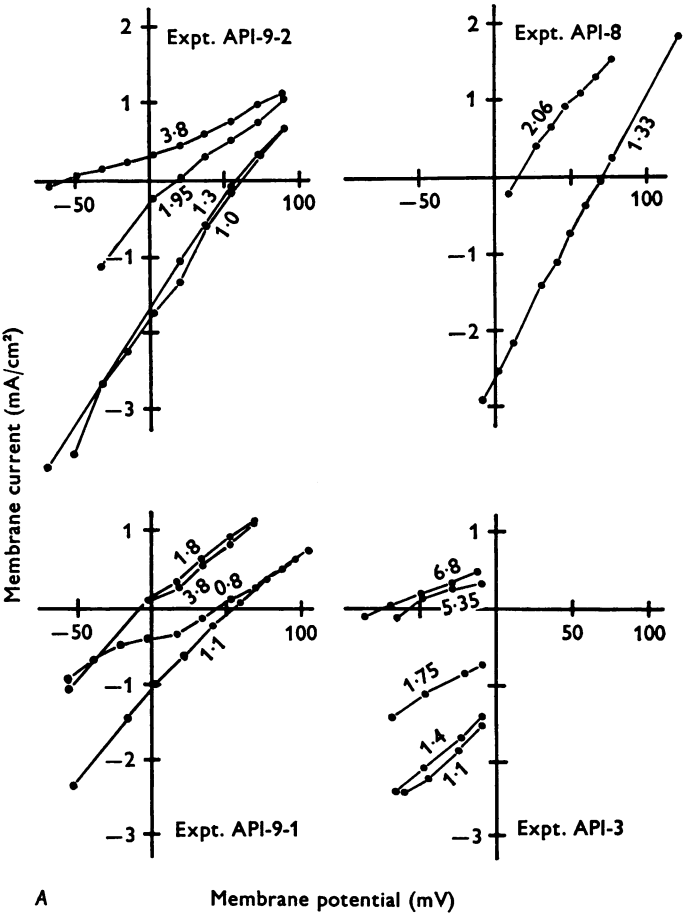

Fig. 5. Instantaneous current–voltage relations during the course of a membrane action potential. *I–V* curves were obtained from frames similar to those shown in Fig. 3. The time at which the membrane potential control was turned on is given next to each *I–V* curve. This time is measured from the initiation of the rectangular pulse of stimulating current. *A*. Instantaneous *I–V* curves for *Dosidicus* axons. The time at which the action potentials reached their peak values were 1·1 msec for API-9-2; 0·9 msec for API-8; 1·13 for API-9-1 and 1·3 for API-3. *B*. Instantaneous *I–V* curves for *Loligo* axon. Times at the peak of the action potentials were 1·0 msec for API-11 and 0·8 msec for API-12.

is an almost linear relationship between current and membrane potential at different times during the action potential.

The usual procedure to obtain an instantaneous current–voltage relation is to plot the logarithm of the current as a function of time and extrapolate back to zero time. We show in the Discussion section of this paper that the

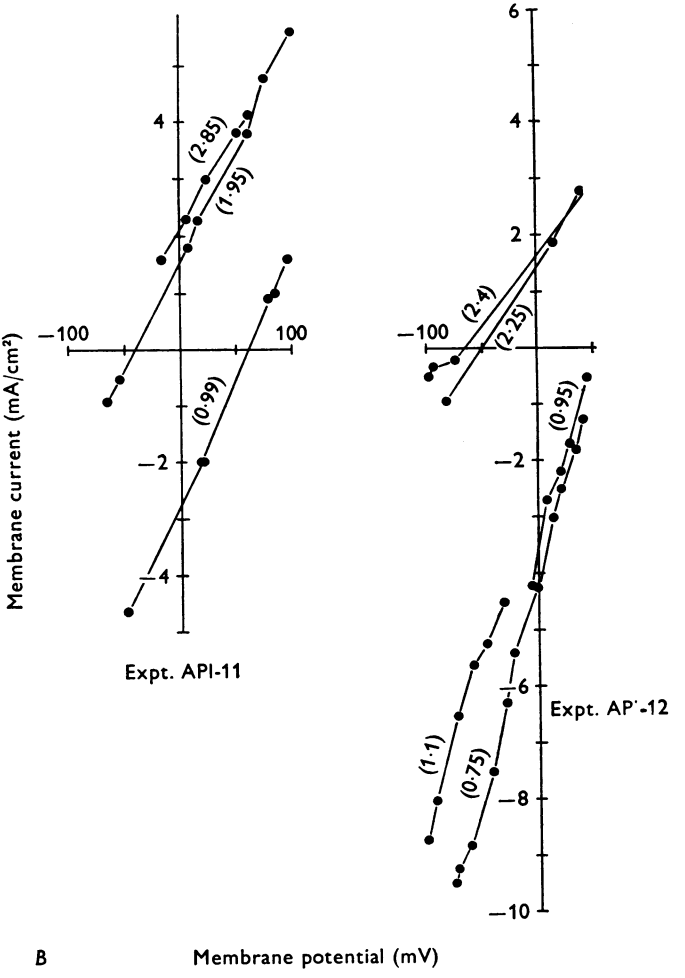

B

Fig. 5*B*. For legend see opposite page.

error introduced by measuring the current 30 μsec after the step change in potential is smaller than 10 %.

These instantaneous current voltage curves are fairly linear at short times when the sodium conductance presumably predominates and at longer times as the potassium conductance takes over from the sodium. For

quantitative comparison between different action potentials it is necessary to take into account the variable stimulus response times. For this reason the time of the peak for each action potential is given in the Figure legend. About 22% of the curves shown in Fig. 5*A* and *B* where taken before the peak of the action potential.

Total conductance change during the course of a membrane action potential

Let us first consider the electrical equivalent circuit for the axon membrane under conditions of space clamp as shown in Fig. 6*A* (Cole, 1968). The equivalent circuit consists of two impedances in series. The first one represents the series resistance and it is generally considered as a pure ohmic component (Hodgkin *et al.* 1952). The second impedance corresponds to the axolemma. This impedance is represented by a capacitor in parallel with several ionic conductive paths, each one of them having its own electromotive force (Hodgkin & Huxley, 1952).

The model can be simplified by replacing all the electrical elements representing different conductive paths by a single conductive path (provided that the instantaneous $I-V$ curves are linear) with only one electromotive force (Condon & Odishaw, 1958; Cole, 1968) as shown in Fig. 6*B*. It can now be shown that it is possible to measure the membrane conductance, G_M, and the open circuit potential, V_T, from the data presented in Fig. 3. The net current through the axolemma is given by

$$I_M = C_M \frac{dV_M}{dt} + I_i \tag{1}$$

where I_M is measured in mA/cm^2, C_M is the capacity of the axolemma measured in μF/cm^2 and I_i is the ionic current measured in mA/cm^2. The current through the axon membrane can be given in terms of conductances and potentials as follows:

$$I_i = (V_M - V_T) G_M, \tag{2}$$

$$I_M = C_M \frac{dV_M}{dt} + (V_M - V_T) G_M, \tag{3}$$

where G_M is the total membrane conductance measured in mmho/cm^2. During a membrane action potential the net current through the axolemma is zero, i.e.

$$I_M = 0 = C_M \frac{dV_M}{dt} + I_i. \tag{1A}$$

When the control system is turned on then, for a controlled potential of V_C (see Fig. 6) and a total current I_C, measured after the capacity transient, the membrane potential during the control period is

$$V_{MC} = V_C - I_C R_S. \tag{4}$$

The total membrane conductance, G_M, is thus given by the ratio of the change in ionic current ($I_C - I_i$ where I_i is calculated with eqn. (1*A*)) divided by the change in membrane potential ($V_{MC} - V_M$ where V_{MC} is given by eqn. (4)) as

$$G_M = (C_M dV_M/dt + I_C)/(V_C - V_M - I_C R_S) \quad (5)$$

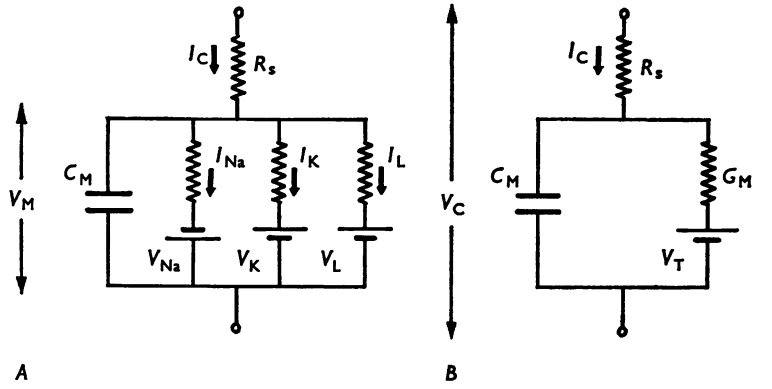

Fig. 6. Equivalent circuits for the axon membrane. Equivalent circuit proposed by Hodgkin & Huxley. R_s represents the series resistance measured in Ω cm^2. I_C represents the current during the voltage clamp and V_C the controlled potential during the clamp. All other symbols have their usual meanings. *B*. For this equivalent circuit all conductances and electromotive forces have been replaced by one conductance, G_M, in series with one electromotive force, V_T.

where again V_M and dV_M/dt are measured from the action potential just before the control system is turned on and I_C is the total current measured after the capacitative current transient. This expression is valid only if G_M (i) is not a function of the membrane potential, and (ii) does not change from the moment in which V_M is measured to the moment when I_C is measured. The first assumption was tested and the results were discussed in the previous section of Results. The second assumption was tested by Hodgkin & Huxley (1952) when they showed that the sodium and the potassium conductances were continuous functions over a step change in membrane potential.

When the potential during the control period takes two different values, V_{C_1} and V_{C_2}, and the corresponding currents I_{C_1} and I_{C_2} are measured, then from eqn. (4) we obtain

$$G_M = \frac{I_{C_2} - I_{C_1}}{V_{C_2} - V_{C_1} - R_s(I_{C_2} - I_{C_1})}. \quad (6)$$

Clearly independent measurements of R_s are required to calculate G_M with either expression (5) or (6). When compensated feed-back is used the determination of G_M with eqn. (6) is immediate.

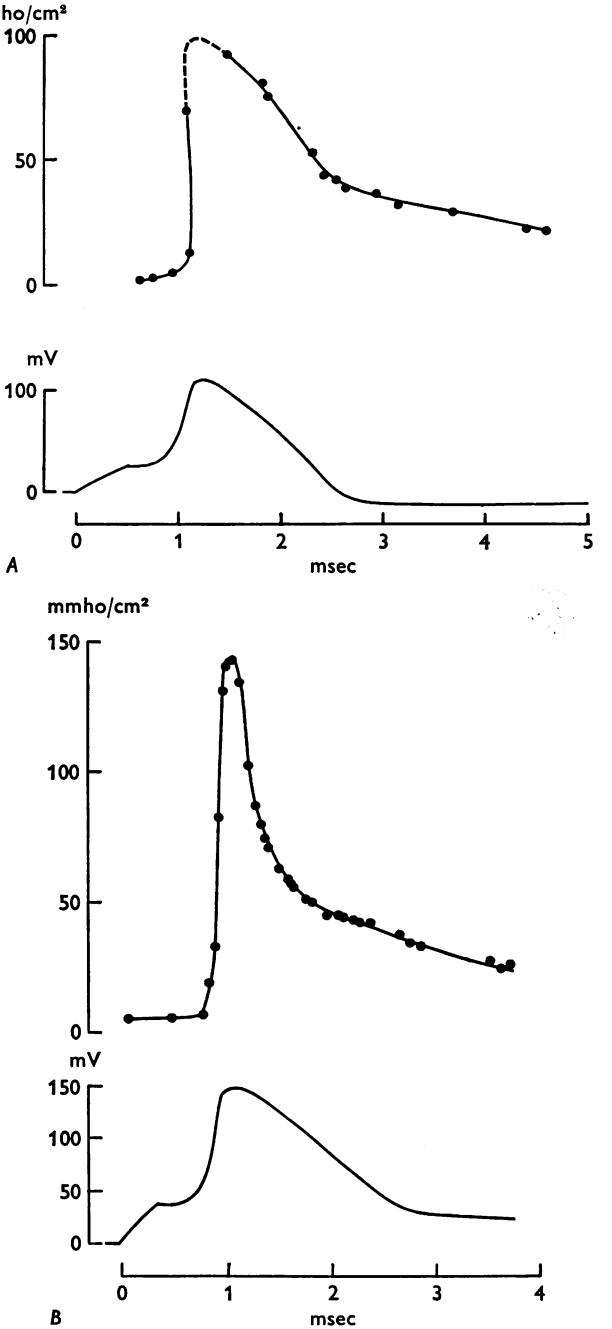

Fig. 7. Total conductance change. *A*. Conductance change calculated with eqn. (5) assuming that C_M is 1·0 μF/cm² and that R_S is equal to 8 Ω cm². Experiment API-11, *Loligo* axon at 10·5° C. *B*. Conductance change calculated with eqn. (6). R_S was taken to be 8 Ω cm². Experiment API-12 *Loligo* axon at 9·5° C.

Fig. 7*A* shows G_M as calculated with eqn. (5) assuming a series resistance of 8 Ω cm² and a membrane capacity equal to 1 μF/cm². Fig. 7*B* shows G_M as calculated with eqn. (6) assuming the same value for R_S. In both experiments uncompensated feed-back was used.

Sodium and potassium conductance change during the course of a membrane action potential

The total membrane conductance can be split into its 'sodium' and 'potassium' components by the following method. If the potential is switched to the potassium reversal potential there is no potassium current and the current is almost entirely in the sodium channel (neglecting a small component of leakage current). The initial values of the ionic current transients are proportional to the sodium conductance change.

Similarly, by switching the membrane potential to the reversal potential of the sodium currents the current is almost entirely in the potassium channel. The initial values of the ionic current transients are proportional to the potassium conductance.

It can be shown that this separation of the sodium and potassium conductances from the total conductance is also possible even if the potential during the voltage clamp period is not the true reversal potential for either the fast or slow channel (see Appendix). After the capacitative current transient is completed the total current is

$$I_C = I_{Na} + I_K + I_L, \tag{7}$$

where I_{Na}, I_K and I_L are the sodium, potassium and leakage current components respectively. This can be expressed in terms of conductances (see Fig. 6*A*):

$$I_C = G_{Na}(V_C - V_{Na} - I_C R_s) + G_K(V_C - V_K - I_C R_s) + G_L(V_C - V_L - I_C R_s),$$

where V_{Na}, V_K and V_L are the reversal potentials for the Na^+, and K^+ and leakage channels respectively (Chandler & Meves, 1965). When V_C takes the value of either V_{Na} or V_K and the series resistance effect is completely compensated, the individual Na^+ and K^+ conductances are immediately calculated provided that G_L and V_L are known. In practice it is difficult to remove the effect of the series resistance completely. This means that when V_C takes the values of either V_{Na} or V_K the calculated conductances have to be corrected. When V_C takes values V^*_{Na} or V^*_K, near V_{Na} or V_K respectively, the conductances G^*_{Na} or G^*_K calculated as

$$G^*_{Na} = \frac{I_C(V^*_K)}{V^*_K - V^*_{Na}}, \tag{8A}$$

$$G^*_K = \frac{I_C(V^*_{Na})}{V^*_{Na} - V^*_K}, \tag{8B}$$

approximately represent the sodium and potassium conductance changes (see Appendix). In these calculations the contribution of the leakage channel and the membrane potential error due to an incomplete compensation are not taken into account. Fig. 8*A* and *B* show results obtained on internally

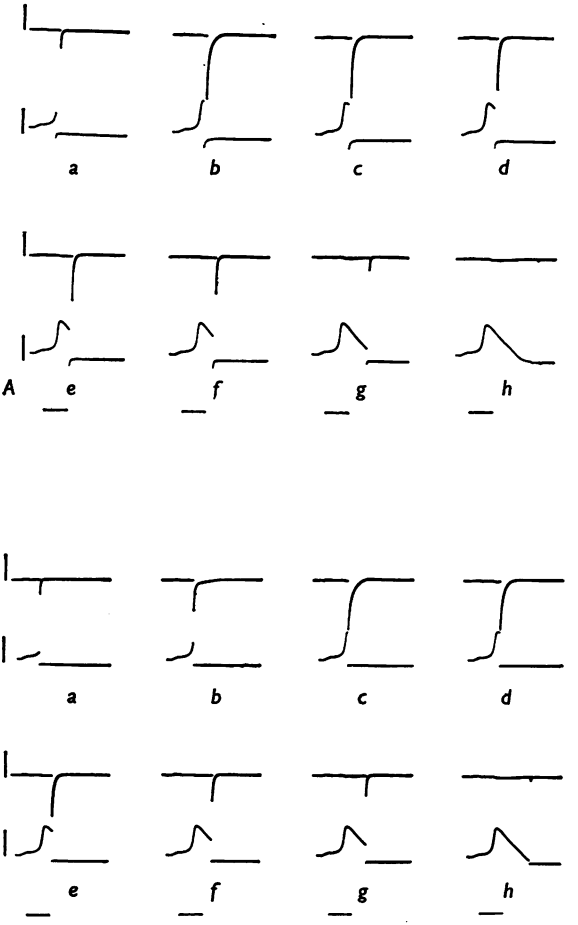

Fig. 8. Action potential interruption to V_K^*. Results obtained with a *Dosidicus* axon. Experiment API-8: Resting potential −65 mV. Temperature 8° C. *A*. Partially compensated feed-back. Calibrations: current: 2·5 mA/cm²; voltage: 100 mV; time: 2 msec. *B*. Uncompensated feed-back. The calibrations are the same as for *A*.

perfused *Dosidicus* fibres when $V_C = V_K^*$. The inward current transients do not all decline with the same rate constant as would be expected in the absence of a series resistance. In those experiments in which compensated feed-back was used (Fig. 8*A*) the rate at which the inward current turns

off is much less dependent on the time at which the voltage clamp was turned on.

Fig. 9 shows the current and membrane potential records when $V_C = V^*_{Na}$ for perfused axons from *Loligo*.

Fig. 10 shows G^*_{Na} and G^*_K obtained utilizing the instantaneous current measured from current records similar to those shown in Figs. 8 and 9. The sodium conductance increases rapidly and reaches its maximum

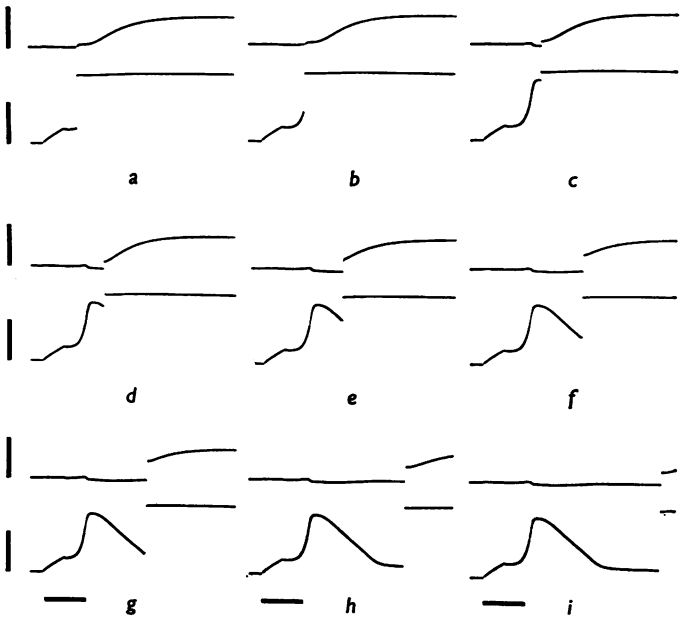

Fig. 9. Action potential interruption to V_{Na}. Results obtained with a *Loligo* axon. Unretouched records from experiment API-12. Resting potential −78 mV. Temperature 9·5° C. Calibrations: current 10 mA/cm²; voltage: 100 mV; time: 1 msec. Uncompensated feed-back. Reversal potential $V_{Na} = +79$ mV. Notice that there is no underswing in this action potential.

value at about the same time at which the action potential is at its peak value; the sodium conductance decrease is slower than the increase. The potassium conductance change starts when the sodium conductance is maximum (upper Fig. 10). However, we think that this displacement of the potassium conductance curve relative to the sodium conductance curve results from the high resting potential of this fibre (−78 mV). Lower Fig. 10 shows the potassium conductance curve relative to the action potential for a different fibre with smaller resting potential (−60 mV).

Comparison with the Hodgkin & Huxley model nerve

The individual ionic conductances shown in Fig. 10 which were calculated utilizing eqn. (8) can be corrected for the effects of the small leakage conductance and of the series resistance (see Appendix). The absolute value of the peak sodium conductance shown in Fig. 10 is slightly larger than the value of 53·4 mmho/cm² calculated by Hodgkin & Huxley (see Table 4, Hodgkin & Huxley, 1952).

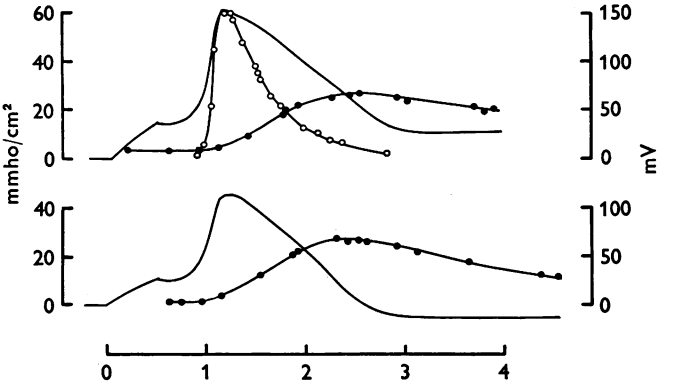

Fig. 10. Temporal course of G^*_{Na} and G^*_K during a membrane action potential. Upper part of this Figure shows the temporal course of G^*_{Na} (open circles) and G^*_K (filled circles) calculated with the uncorrected data from experiment API-12. Temperature 9·5° C. Resting potential −78 mV. Lower part of this Figure shows G^*_K calculated with the data obtained on a *Loligo* axon. Resting potential −64 mV. Notice the underswing in the action potential.

Sodium and potassium conductances change with the different conditions taken into account during the calculation. In comparing the time course and the size of the potassium conductance relative to the size of the sodium conductance it is convenient to normalize both calculated and measured conductances. Accordingly the data shown in Fig. 10 were normalized after corrections for leakage conductance and series resistance. The calculated conductance at 10° C have been normalized and they are compared with the experimental results in Fig. 11. For these calculations only the initial conditions were changed to take into account the high resting potential measured in this particular fibre.

The rapid rise of both the calculated and measured sodium conductance is almost identical and occurs almost at the same time. The fall off of the experimental sodium conductance, however, is faster than the calculated fall off.

The time course of both potassium conductances is very similar and the ratio peak G_K/peak G_{Na} for the experimental curve compares well with the same ratio for the calculated data. After the peak of the sodium conductance the potassium conductance takes a progressively larger share. The interval

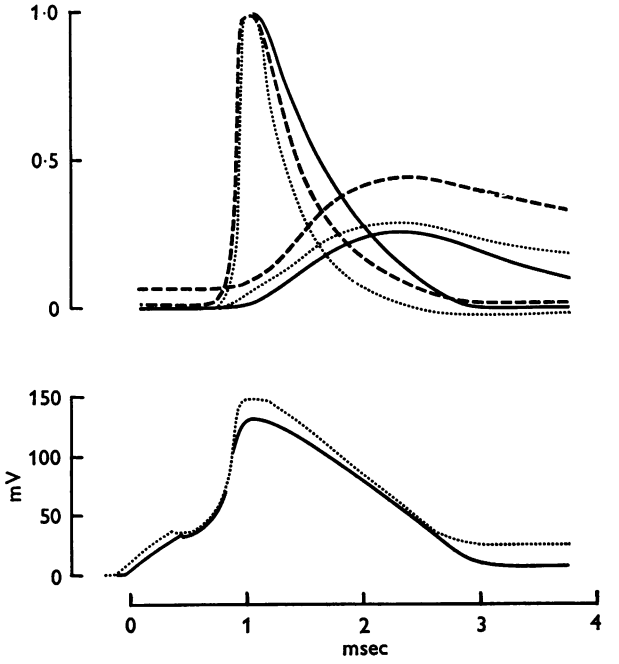

Fig. 11. Comparison with the G_{Na} and G_K as calculated with the Hodgkin & Huxley equations. Upper figures represent normalized sodium and potassium conductances. The maximum sodium conductance in each case was considered as one. Dashed lines: normalized G^*_{Na} and G^*_K for experiment API-12. Dotted lines: normalized sodium and potassium conductances corrected for a leakage conductance of 5 mmho/cm² and a series resistance of 8 Ω cm² following eqns. (3) and (4) in the Appendix. The continuous lines are the Hodgkin & Huxley corresponding G_{Na} and G_K. These were computed increasing the resting potential 20 mV by having a constant 9·2 μA/cm² hyperpolarizing current. Temperature 10° C. Lower curves represent the tracings of the measured membrane potential (dotted curve) and the calculated one (continuous curve). The measured action potential has been displaced towards the left so that the peaks of both action potentials occur at the same time.

between the sodium and potassium conductance peaks is dependent on the initial conditions, particularly the resting potential (Cole & Moore, 1960). Thus the onset of the potassium conductance is delayed as the resting potential increases. For a 20 mV hyperpolarization the equations predict an increase of the interval between the sodium and potassium peak of

about 250 μsec. This same increase was measured utilizing the potassium conductance curves shown in Fig. 10 which were obtained on two fibres with different resting potentials (-78 mV and -64 mV).

DISCUSSION

Validity of the method

First, it is necessary to clarify what is meant by separation of individual ion conductances from the total membrane conductance. Then we may ask about the properties of the system which may introduce errors in the determination of relevant quantities. We have used the approach of Hodgkin, Huxley & Katz (1952) where it is first assumed that the different ions flow through the membrane independently. Except for active transport (Baker, Blaustein, Keynes, Manil, Shaw & Steinhardt, 1969) no experimental evidence for interactions have appeared. We may take the equivalent circuit shown in Fig. 6 as being generally valid as a kind of spatial average, since it is difficult to believe that the membrane is a uniform structure. The mosaic nature of the membrane also leads to the uncertainty that the resistance in series with the membrane capacitance is the same at different points or for different ionic pathways. Difficulties arise not with the equivalent circuit but with the question of the dependence of the parameters on voltage, time and current flow. In the Hodgkin–Huxley equations the individual ion conductance terms do not vary with membrane potential for times short compared to the delays associated with their equations. This is an experimentally approachable question of some importance. The results which we have presented give very strong support to the conclusion that for axons of *Dosidicus* or *Loligo* the 'instantaneous' current–voltage relations are linear. The method for separating these conductances presented here depends on this linearity. If for other excitable membranes the curves were not linear new definitions would be needed (cf. Frankenhaeuser, 1960; Dodge & Frankenhaeuser, 1959). For example, the slope conductance at zero current might be used as a parameter and if the current–voltage curves at various times had the same shape the quantities measured by suddenly controlling the membrane potential to V_K or V_{Na}, essentially chord conductances, would be proportional to this parameter.

It is not appropriate to discuss the matter at length here but it should be mentioned that the 'sodium conductance' refers to the conductance for ions passing through a channel with certain properties whether or not sodium happens to be the ion carrying the current. For the experiments presented here the axons were perfused with potassium fluoride. It is known that potassium flows through the sodium channel with about 1/10 to 1/25 the ease of sodium ions (Chandler & Meves, 1965; Rojas & Atwater,

1967). Thus for these measurements the situation for the sodium channels is equivalent to an internal sodium concentration which is some fraction of the existing potassium concentration. Similar considerations apply to the potassium conductance.

Effects of series resistance

As mentioned above it is not known if the series resistance as shown in Fig. 6 is the same for the sodium and potassium channels but this is a refinement which we cannot consider here. We may ask about the effects of this series resistance or we may attempt to compensate for it by electronic means or try to correct the data by computation (which is not always uniquely possible; see Taylor, Moore & Cole, 1960).

Negative resistance compensation. It is possible partially to compensate for a series resistance (see Hodgkin *et al.* 1952) electronically as shown in the circuit diagram in Fig. 2. Analyis of the stability properties of the system shown in Fig. 2 has not been done to our knowledge and the best we can do at the present is to compare the measured current (I_C) with the deviation of the time course of the clamped potential (V_C). If R_s is a pure resistance and the system is working properly they should be proportional.

Let us consider the results when the potential during the voltage clamp period is equal to the reversal potential for the potassium channels. Fig. 8*A* and *B* show the results obtained with incomplete compensation and without compensation. Uncompensated series resistance reduces the magnitude of the initial transient of sodium current and also decreases the rate at which the sodium current turns off. Some records even show a delay of this sodium current turn off. This delay seems to be different depending on the initial magnitude of the currents.

The effects of the series resistance upon the membrane current transients were studied by solving the Hodgkin–Huxley equations under conditions similar to the experimental situations. It is assumed that the change in membrane potential from its value before the voltage clamp system is turned on follows an exponential time course with a time constant τ_C. Fig. 12 shows some of the results. τ_C was chosen equal to 1 μsec and the series resistance was varied from 0 to 50 Ω cm^2. The usual analytical solutions of the Hodgkin–Huxley equations would correspond to a fully compensated system and an instantaneous membrane potential change. The case labelled 0 Ω cm^2 in Fig. 12 for the membrane potential change with time constant of 1·0 μsec is close to this.

It is apparent that the series resistance has a very marked effect on the amplitude and duration of the capacitative transient, and also upon the duration and amplitude of the ionic currents. Some of these effects were experimentally observed. For a very large series resistance the sodium tail

may exhibit a hump as demonstrated by the curve for 50 Ω cm² in Fig. 12. Although such large series resistances have not been reported for squid giant axons similar effects could arise for axons with very large conductances.

If in Fig. 12 we take the curves representing ionic currents and we extrapolate them to the time zero and these extrapolated currents are

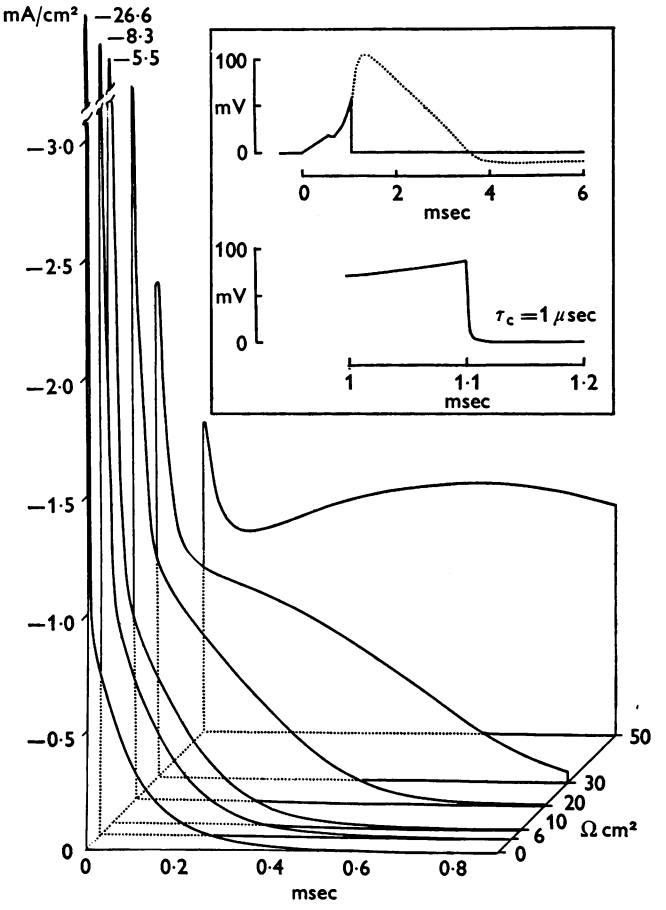

Fig. 12. I_C-t-R_s diagram showing the effects of the series resistance on current transients as computed using the Hodgkin & Huxley equations. Conditions used to solve the equations are given in the insert. The action potential was interrupted 1·1 msec after the application of the stimulating current. (Dotted line shows uninterrupted action potential.) Lower part of insert is expanded time scale around moment of interruption. Response characteristic of voltage clamping system is represented by an exponential time constant of 1·0 μsec for V_C after interruption. Maximum inward current given by numbers of the top of first three transients.

compared with the initial currents obtained with the equations for a perfect step in membrane potential, no serious discrepancies are observed for a series resistance of less than 6 Ω cm^2. Thus our measurements should be close to the instantaneous ionic currents even without complete series resistance compensation.

Comparison with earlier results and predictions

Our results concerning the total conductance change during the action potential agree fairly well with the measured conductance change demonstrated by Cole & Curtis in 1939. We did not try to make quantitative comparisons between their results and ours because we measured the conductance change during a membrane action potential and the Cole & Curtis measurements were made during a propagated action potential. However, the shape of the conductance curve as a function of time in our measurements shows the same features and approximately the same time relationship with the membrane potential as their results.

The temporal course of the sodium and potassium conductances are very similar to those predicted by the H–H equations (see Fig. 11). The major differences are that the experimental sodium conductance decreases faster and that the experimental potassium conductance recovers slower than predicted by the equations. We have seen better agreement in the sodium conductance fall off in other axons but the potassium decay was slower in all cases. Considering that the major features of the experimental conductance changes are very well reproduced by the equations we concluded that they are a very good description of the membrane behaviour during excitation.

We wish to thank Professor A. L. Hodgkin and Dr Kenneth S. Cole for reading and commenting on this paper. This work was supported by the University of Chile and by the U.S. National Institutes of Health under grant NB-06503-03. Computations were carried out while F. B. was a visiting Fellow at the U.S.A. National Institutes of Health.

APPENDIX

Separation of the conductances

When the potential during the control period is different from the true reversal potentials (either V_{Na} or V_K) it is still possible to split the total conductance into its components.

For interruptions of the membrane action potential to V^*_{Na} and V^*_K then using eqn. (8) of the text we can write:

$$G_{Na}(V^*_{Na}-I_1R_s-V_{Na})+G_K(V^*_{Na}-I_1R_s-V_K)=I_1-G_L(V^*_{Na}-I_1R_s-V_L), \quad (1)$$

$$G_{Na}(V^*_K-I_2R_s-V_{Na})+G_K(V^*_K-I_2R_s-V_K)=I_2-G_L(V^*_K-I_2R_s-V_L), \quad (2)$$

where I_1 and I_2 are the instantaneous ionic currents during the potential control period at V^*_{Na} and V^*_K respectively. To solve eqns. (1) and (2) it is necessary to know the values of G_L, V_{Na}, V_K, V_L and R_s. These five parameters may be determined in regular voltage clamp and current clamp runs.

Solving eqns. (1) and (2) for G_{Na} and G_K we get

$$G_{Na} = \frac{(V^*_K - V_{Na})(K_1 - I_1) + (V_{Na} - V^*_{Na})(K_2 - I_2) + R_s(K_2 I_1 - K_1 I_2)}{(V_{Na} - V_K)[R_s(I_2 - I_1) + (V^*_{Na} - V^*_K)]}, \quad (3)$$

$$G_K = \frac{(V^*_K - V_{Na})(K_1 - I_1) + (V_{Na} - V^*_{Na})(K_2 - I_2) + R_s(K_2 I_1 - K_1 I_2)}{(V_{Na} - V_K)[R_s(I_2 - I_1) + (V^*_{Na} - V^*_K)]}, \quad (4)$$

where K_1 and K_2 are defined as follows:

$$K_1 = G_L(V^*_{Na} - I_1 R_s - V_L), \quad (5)$$

$$K_2 = G_L(V^*_K - I_2 R_s - V_L). \quad (6)$$

When $V^*_{Na} = V_{Na}$, $V^*_K = V_K$ and the series resistance has been fully compensated, neglecting the leakage conductance eqns. (3) and (4) give $G^*_{Na} = G_{Na}$ and $G^*_K = G_K$ where G^*_{Na} and G^*_K have been defined in eqns. (8A) and (8B) of the text.

REFERENCES

ATWATER, I., BEZANILLA, F. & ROJAS, E. (1969). Sodium influxes in internally perfused squid giant axon during voltage clamp. *J. Physiol.* **201**, 657–664.

BAKER, P. F., BLAUSTEIN, M. P., KEYNES, R. D., MANIL, J., SHAW, T. I. & STEINHARDT, R. A. (1969). The ouabain-sensitive fluxes of sodium and potassium in squid giant axon. *J. Physiol.* **200**, 459–496.

BEZANILLA, F., ROJAS, E. & TAYLOR, R. E. (1970). Time course of the sodium influx in squid giant axon during a single voltage clamp pulse. *J. Physiol.* **207**, 151–164.

CHANDLER, W. K. & MEVES, H. (1965). Voltage clamp experiments on internally perfused giant axons. *J. Physiol.* **180**, 788–820.

COLE, K. S. (1968). *Membrane, Ions and Impulses.* Berkeley California: University of California Press.

COLE, K. S. & CURTIS, H. J. (1939). Electric impedance of the squid giant axon during activity. *J. gen. Physiol.* **22**, 649–670.

COLE, K. S. & MOORE, J. W. (1960). Potassium ion current in the squid giant axon: Dynamic characteristic. *Biophys. J.* **1**, 1–14.

CONDON, E. V. & ODISHAW, H. (1958). *Handbook of Physics.* New York: McGraw-Hill Book Company Inc.

DODGE, F. A. & FRANKENHAEUSER, B. (1959). Sodium currents in the myelinated nerve fibre of *Xenopus laevis* investigated with the voltage clamp technique. *J. Physiol.* **148**, 188–200.

FRANKENHAEUSER, B. (1960). Sodium permeability in toad nerve and in squid nerve. *J. Physiol.* **152**, 159–166.

HODGKIN, A. L. & HUXLEY, A. F. (1952). A quantitative description of membrane current and its application to conduction and excitation in nerve. *J. Physiol.* **117**, 500–544.

HODGKIN, A. L. & HUXLEY, A. F. (1952). The components of membrane conductance in the giant axon of *Loligo*. *J. Physiol.* **116**, 473–496.

HODGKIN, A. L., HUXLEY, A. F. & KATZ, B. (1952). Measurement of current–voltage relations in the membrane of the giant axon of *Loligo*. *J. Physiol.* **116**, 424–448.

MORLOCK, N. L., BENAMY, D. A. & GRUNDFEST, H. (1968). Analysis of spike electrogenesis of eel electroplaques with phase plane and impedance measurements. *J. gen. Physiol.* **52**, 22–45.

PEPER, K. & TRAUTWEIN, W. (1969). A note on the pacemaker current in purkinje fibers. *Pflugers Arch. ges. Physiol.* **309**, 356–361.

ROJAS, E. & ATWATER, I. (1967). Effect of tetrodotoxin on the early outward currents in perfused giant axons. *Proc. natn. Acad. Sci. U.S.A.* **57**, 1350–1355.

ROJAS, E., BEZANILLA, F. & TAYLOR, R. E. (1970). Demonstration of sodium and potassium conductance changes during a nerve action potential. *Nature, Lond.* **225**, 747–748.

ROJAS, E., TAYLOR, R. E., ATWATER, I. & BEZANILLA, F. (1969). Analysis of the effects of calcium or magnesium on voltage-clamp currents in perfused squid axons bathed in solutions of high potassium. *J. gen. Physiol.* **54**, 532–552.

TAYLOR, R. E., MOORE, J. W. & COLE, K. S. (1960). Analysis of certain errors in squid axon voltage clamp measurements. *Biophys. J.* **1**, 161–202.

VASALLE, M. (1966). Analysis of cardiac pacemaker potential using a 'voltage clamp' technique. *Am. J. Physiol.* **210**, 1335–1341.

WEIDMANN, S. (1951). Effect of current flow on the membrane potential of cardiac muscle. *J. Physiol.* **115**, 227–236.